

STRPM: A Spatiotemporal Residual Predictive Model for High-Resolution Video Prediction

Zheng Chang^{1,2}, Xinfeng Zhang¹, Shanshe Wang^{3*}, Siwei Ma³, and Wen Gao^{1,3}

¹School of Computer Science and Technology,

University of Chinese Academy of Sciences, Beijing, China

²Institute of Computing Technology, Chinese Academy of Sciences, Beijing, China

³National Engineering Research Center of Visual Technology,

School of Computer Science, Peking University, Beijing, China

changzheng18@mails.ucas.ac.cn, xfzhang@ucas.ac.cn, {sswang, swma, wgao}@pku.edu.cn

Abstract

Although many video prediction methods have obtained good performance in low-resolution (64~128) videos, predictive models for high-resolution (512~4K) videos have not been fully explored yet, which are more meaningful due to the increasing demand for high-quality videos. Compared with low-resolution videos, high-resolution videos contain richer appearance (spatial) information and more complex motion (temporal) information. In this paper, we propose a Spatiotemporal Residual Predictive Model (STRPM) for high-resolution video prediction. On the one hand, we propose a Spatiotemporal Encoding-Decoding Scheme to preserve more spatiotemporal information for high-resolution videos. In this way, the appearance details for each frame can be greatly preserved. On the other hand, we design a Residual Predictive Memory (RPM) which focuses on modeling the spatiotemporal residual features (STRF) between previous and future frames instead of the whole frame, which can greatly help capture the complex motion information in high-resolution videos. In addition, the proposed RPM can supervise the spatial encoder and temporal encoder to extract different features in the spatial domain and the temporal domain, respectively. Moreover, the proposed model is trained using generative adversarial networks (GANs) with a learned perceptual loss (LP-loss) to improve the perceptual quality of the predictions. Experimental results show that STRPM can generate more satisfactory results compared with various existing methods.

*Corresponding author: Shanshe Wang, sswang@pku.edu.cn. This work was supported in part by the National Natural Science Foundation of China (62025101, 62072008, 62071449, U20A20184), National Key Research and Development Project of China (2019YFF0302703, 2021YFF0900503) and High-performance Computing Platform of Peking University, which are gratefully acknowledged.

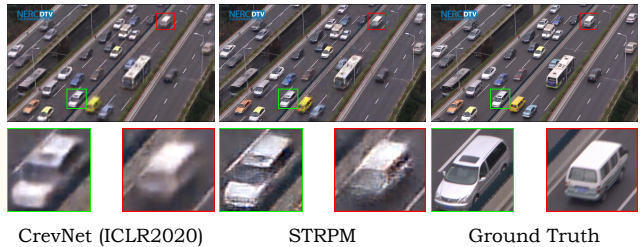


Figure 1. Qualitative results between the proposed STRPM and the state-of-the-art method CrevNet [29] on the SJTU4K dataset (4K: 2160×3840 resolution, 4 frames → 1 frame). STRPM has generated much better visual details compared with CrevNet.

1. Introduction

Video prediction is a key component of representation learning due to its great ability in modeling meaningful representations for natural videos and has been applied to various video processing applications, such as video coding [14], precipitation nowcasting [20], robotic control [6], autonomous driving [2] and so on. Different from video interpolation [16, 17], video prediction (extrapolation) is more challenging by merely utilizing limited information from previous frames to predict the unknown future frames. Motivated by the advantages of deep learning technologies in extracting deep features, in recent years, various learning-based methods have been proposed for video prediction which can be summarized into three types.

The first type of methods [20, 22, 25–27, 29] utilize Recurrent neural networks (RNN) to progressively predict video frames due to their unique advantages in sequence learning and have obtained some satisfactory results. However, the predictions from RNN-based methods are typically blurry due to the standard mean square error based loss function. To solve this problem, the second type of meth-

ods [1, 5, 7, 23, 28] utilize deep stochastic models to predict different futures instead of an averaged future for different samples and the third type of methods [4, 8, 12, 13, 15] employ generative adversarial networks (GANs) [8] and additional perceptual loss functions to augment the visual qualities of the predictions.

Although the above methods have obtained some satisfactory results, the resolutions of video datasets utilized in the above methods are usually low (64~128), and the performance in high-resolution (512~4K) videos is still hardly satisfactory (shown in Figure 1), preventing their adaptability and practicability into real scenarios. There are mainly two challenges restricting the resolution of predictions. The first challenge is that high-resolution videos usually contain more complex visual details. However, limited by the computation resources, videos are usually encoded to low-dimensional features and then decoded back to the video frames, during which, lots of visual details can be abandoned. The second challenge is that the motion information in high-resolution videos typically involves multiple objects, which is much more complex and hard for traditional predictive memory to predict. To deal with the above two problems in high-resolution video prediction, the appearance information in the spatial domain and the motion information in the temporal domain need to be carefully reconsidered.

In this paper, we propose a Spatiotemporal Residual Predictive Model (STRPM) to deal with the above two challenges. Firstly, to predict more satisfactory appearance details for each frame, we novelly propose the spatiotemporal encoding-decoding scheme, which utilizes independent encoders to extract deep features in both spatial and temporal domains. In this way, both the spatial and temporal information can no longer affect each other and more visual details can be preserved. Secondly, to accurately model the complex motion information in high-resolution videos, we designed a Residual Predictive Memory (RPM) to focus on modeling the inter-frame spatiotemporal residual features (STRF) with a relatively low computation load and fewer parameters. Moreover, since the encoded spatial and temporal features will be fed into the spatial and temporal modules in RPM for transitions in vertical (spatial domain) and horizontal (temporal domain) directions, the RPM can indirectly supervise the spatial encoder and the temporal encoder to extract corresponding features in the spatial domain and the temporal domain.

By jointly using the encoded spatiotemporal features and STRF, more reliable spatiotemporal features for future frames can be predicted, which will be further decoded back to the high-dimensional data space with the help of spatiotemporal decoders. Furthermore, in the training stage, the standard MSE loss, the adversarial loss as well as the learned perceptual loss are jointly utilized to improve the

visual quality of the predictions. Experimental results show that the proposed model can achieve state-of-the-art performance compared with other methods.

2. Related Work

In recent years, many learning-based predictive models have been applied in video prediction. [18] first utilized language modeling for video prediction, which was further improved by [22] using Long Short-Term Memories (LSTMs) [9], denoted as FC-LSTM. To improve the model perception to visual data, [20] integrated convolutional operations to FC-LSTMs (ConvLSTM) and achieved significant improvements on the Moving MNIST dataset.

However, the above works only focus on the inter-frame temporal information (motion information) and ignored intra-frame spatial information (appearance information). To preserve the appearance information for videos, [26] designed an appearance-preserving block for ConvLSTM (PredRNN). [24] further improved PredRNN by solving the gradient propagation difficulties in deep predictive models (PredRNN++) and integrating 3D convolution operations and RECALL gate to enhance the ability to capture both long-term and short-term dependencies of the predictive model (E3D-LSTM). To further improve the visual quality of the predictions, [29] proposed a conditionally reversible network (CrevNet) to preserve the spatiotemporal information for the inputs and [11] leveraged the high-frequency information to preserve visual details for videos.

However, the above works can only generate an averaged future for all samples due to the standard MSE loss function and the predictions are usually blurry. To solve this problem, a variety of methods have been proposed. On the one hand, some methods aim to predict different futures for different samples. [1] proposed a stochastic variational video prediction (SV2P) method to predict a different possible future for each sample based on the latent variables. [5, 28] proposed video generation models with a learned prior over stochastic latent variables for video prediction. [7] proposed a stochastic temporal model for video prediction whose dynamics are governed in a latent space by a residual update rule.

On the other hand, some works aim to improve the standard MSE-based loss function. [15] proposed three different and complementary feature learning strategies to predict naturalistic videos. Besides, motivated by the great power in generating naturalistic images, generative adversarial networks (GANs) were employed by [13] to generate realistic results and [12] utilized CycleGAN [31] to further improve the perceptual quality of the predictions. Although some improvements have been achieved in above works and the resolutions of the predicted videos have been improved in [3, 29] (256~512), the unacceptable computation load and quality distortions prevent them from predicting

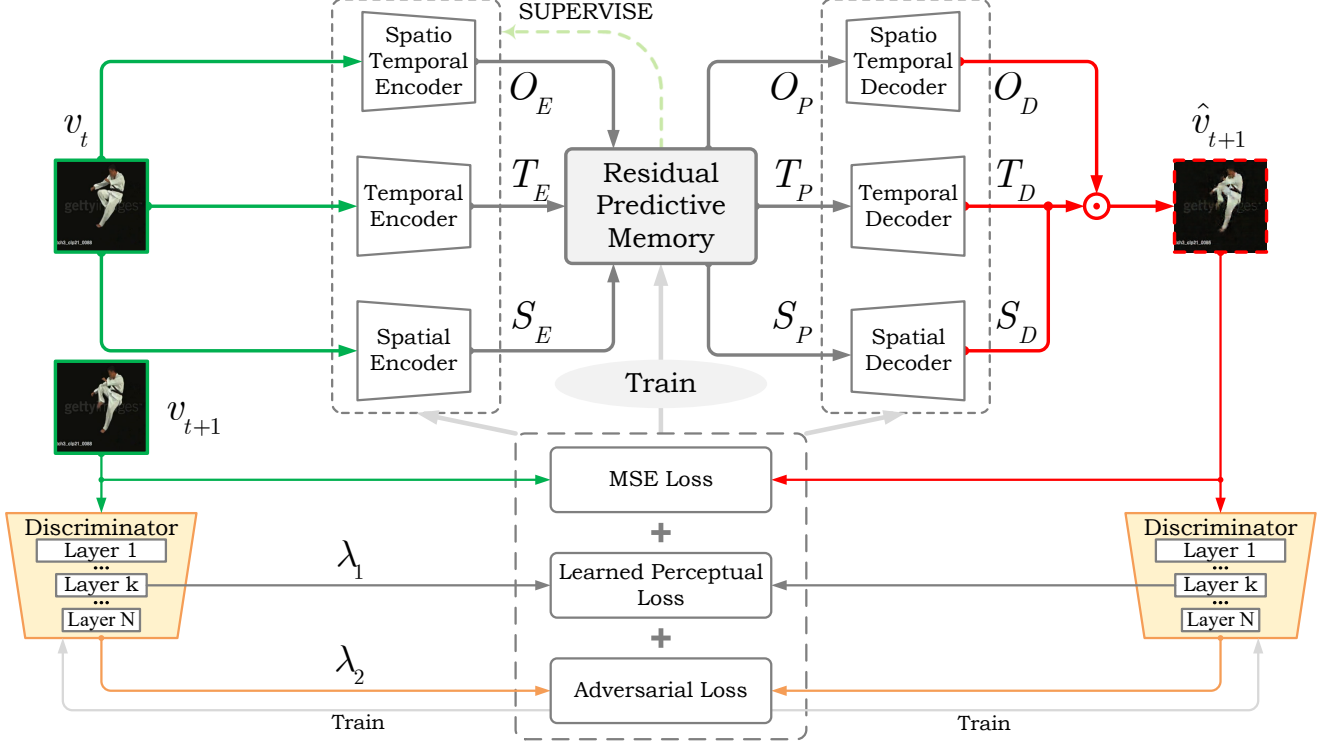


Figure 2. The structure of the proposed spatiotemporal residual predictive model (STRPM). The green arrows denote the input information flows and the red arrows denote the predicted information flows.

videos with higher resolution (512~4K). To solve the above problems, we propose a spatiotemporal residual predictive model (STRPM) for high-resolution video prediction with an acceptable computation load. Moreover, by using the proposed learned perceptual loss, more naturalistic videos can be generated from the proposed method.

3. The Spatiotemporal Residual Predictive Model

In this section, we introduce the proposed Spatiotemporal Residual Predictive Model (STRPM) in detail. The overall structure of the proposed model is shown in Figure 2. Different from low-resolution videos, high-resolution videos contain more complex texture details and more variable motion information, motivated by which, two problems for high-resolution video prediction urgently need to be solved:

- How to preserve more visual details for each frame?
- How to predict more accurate motion information between frames?

We propose the Spatiotemporal Residual Predictive Model (STRPM) to solve the above problems.

3.1. Spatiotemporal Encoding-Decoding Scheme

To reduce the computation resources, video frames are typically encoded to low-dimensional features using a single encoder in video prediction. However, the temporal information and the spatial information will affect each other and the predictive memories have to further extract the temporal and spatial information to predict future frames, during which, lots of spatiotemporal information may be lost, making it very difficult to reconstruct satisfactory visual details for each frame. To solve this problem (the first problem), we novelly utilize multiple spatiotemporal encoders to independently extract deep features in both temporal and spatial domains. In this way, the spatial information and the temporal information will no longer affect each other, making it easier for the predictive memories to utilize the spatiotemporal information for video prediction. The encoding process can be expressed as follows,

$$(T_E, S_E, O_E) = (Enc_T(v_t), Enc_S(v_t), Enc_O(v_t)), \quad (1)$$

where v_t denotes the t^{th} frame in source video V . $Enc_T(\cdot)$, $Enc_S(\cdot)$, $Enc_O(\cdot)$ denote the temporal, spatial and spatiotemporal encoders respectively. T_E , S_E , O_E denote the encoded low-dimensional temporal, spatial and spatiotemporal features at time step t , respectively.

In particular, the above encoded features T_E , S_E , O_E

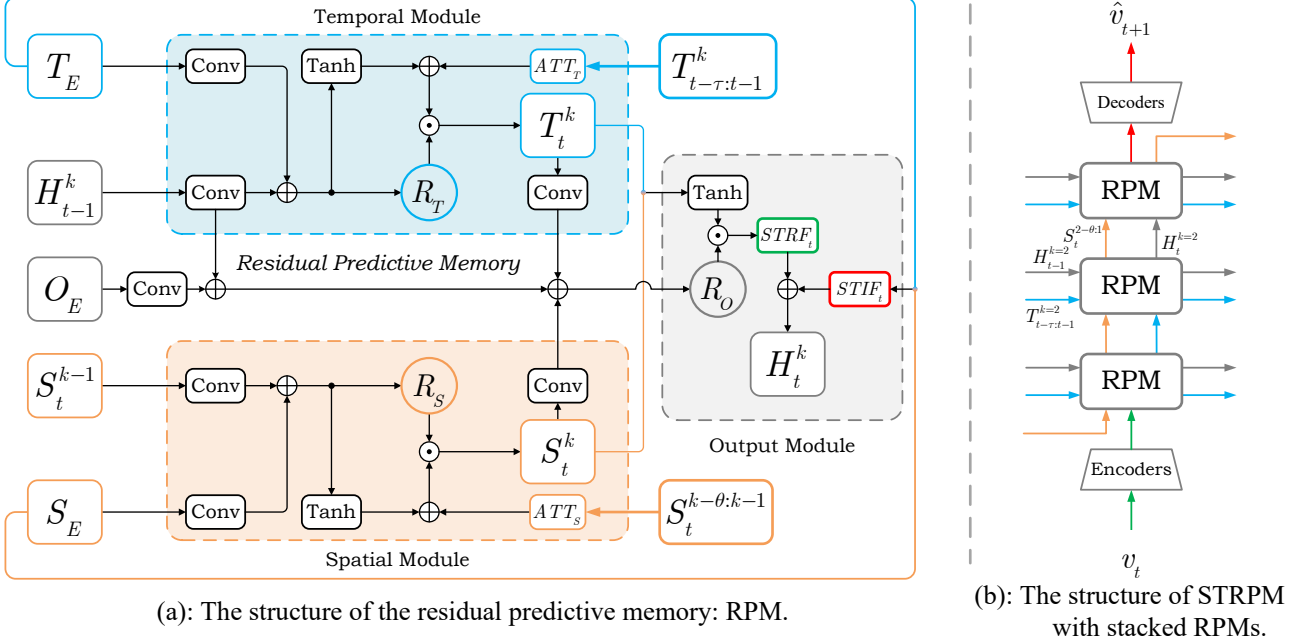


Figure 3. The structure of the proposed residual predictive memory: RPM. The temporal module and the spatial module can indirectly supervise the temporal encoder and the spatial encoder to extract different features in the temporal domain and the spatial domain.

will be fed into the corresponding modules in the proposed residual predictive memory: RPM, which will be detailedly introduced in section 3.2. In this way, the RPM can indirectly supervise different encoders to extract different features in different domains. And the predicted spatiotemporal features can be represented as follows,

$$(T_P, S_P, O_P) = \text{RPM}(T_E, S_E, O_E, \mathcal{T}, \mathcal{S}), \quad (2)$$

where T_P, S_P, O_P denote the predicted temporal, spatial and spatiotemporal features at time step t from RPM, respectively. \mathcal{T}, \mathcal{S} are the preserved temporal and spatial information.

Similar as the encoding process, to decode more spatiotemporal details, we also utilize multiple spatiotemporal decoders to decode the predicted features from low-dimensional feature space back to high-dimensional temporal and spatial data space respectively, which can be expressed as follows,

$$(T_D, S_D, O_D) = (\text{Dec}_T(T_P), \text{Dec}_S(S_P), \text{Dec}_O(O_P)), \quad (3)$$

where $\text{Dec}_T(\cdot), \text{Dec}_S(\cdot), \text{Dec}_O(\cdot)$ denote the temporal, spatial and spatiotemporal decoders, respectively. T_D, S_D, O_D denote the decoded high-dimensional temporal, spatial and spatiotemporal features, respectively.

By jointly utilizing the decoded high-dimensional features, the predicted frame at time step t can be represented as follows,

$$\hat{v}_{t+1} = O_D \odot \tanh(W_{1 \times 1} * [T_D, S_D]), \quad (4)$$

where \hat{v}_{t+1} denotes the predicted frame at time step t , $\odot, *$ denote the hadamard product and convolutional operators.

3.2. The Residual Predictive Memory: RPM

Current predictive memories aim to predict future frames by learning a single representation for the whole frame, containing both the spatial representation and the temporal representation, which is efficient to predict simple motions. However, high-resolution videos usually contained much more complex motion information compared with low-dimensional videos. To deal with this special characteristic in high-resolution videos (the second problem), we design a Residual Predictive Memory (RPM) to focus on modeling inter-frame motion information by predicting the spatiotemporal residual features (STRF) between previous and future frames in the feature space, which is shown in Figure 3(a). In addition, compared with traditional ST-LSTM structure [26], the proposed RPM also benefits from more efficient state-to-state transitions (fewer gates) and wider spatiotemporal receptive field (simultaneously utilizing multiple spatiotemporal states). To further extract more efficient deep spatiotemporal features, multiple RPMs are typically stacked into a single model, as shown in Figure 3(b). For RPM at time step t in layer k , the encoded features T_E, S_E, O_E are fed into the corresponding modules of RPM. In this way, the proposed RPM can indirectly supervise the spatial encoder and the temporal encoder to extract different deep features in the spatial domain and the temporal domain. In particular, for $k > 1$, the encoded fea-

tures are represented with the hidden state from the previous layer, i.e., $T_E, S_E, O_E = H_t^{k-1}$.

For each RPM, there are seven inputs: T_E , the encoded features for the temporal module; S_E , the encoded features for the spatial module; O_E , the encoded spatiotemporal features for the output module; H_{t-1}^k , the hidden state from previous time step; S_t^{k-1} , the previous spatial state from previous layer $k-1$; $\mathcal{T} : T_{t-\tau:t-1}^k$, the previous τ temporal states; $\mathcal{S} : S_{t-\theta:k-1}^k$, the previous θ spatial states. To further improve local perception to videos, the input states are typically preprocessed using convolutional layers:

$$\begin{aligned} (TF_t^k, SF_t^k, OF_t^k) &= (W_t * T_E, W_s * S_E, W_o * O_E), \\ (HF_t^k, MF_t^k) &= (W_h * H_{t-1}^k, W_m * S_t^{k-1}), \end{aligned} \quad (5)$$

where W denotes the parameters of the integrated convolutional layers. $TF_t^k, SF_t^k, OF_t^k, HF_t^k, MF_t^k$ denote the extracted deep features from $T_E, S_E, O_E, H_{t-1}^k, S_t^{k-1}$, respectively. Then the extracted features will be fed into RPM at time step t in layer k .

For both the temporal and spatial module, two residual gates are designed to model the inter-frame residual information, which is shown as follows,

$$\begin{aligned} R_T &= \sigma(TF_t^k + HF_t^k), \\ R_S &= \sigma(SF_t^k + MF_t^k), \end{aligned} \quad (6)$$

where R_T, R_S denote the temporal and spatial residual gates, respectively.

As shown in Figure 3(a), the temporal module (blue block) of RPM is utilized to capture reliable motion information between frames. To preserve more useful temporal information from the past, RPM jointly utilizes multiple temporal states, and the transitions can be expressed as follows,

$$T_t^k = R_T \odot (\tanh(TF_t^k + HF_t^k) + ATT_T(\mathcal{T})). \quad (7)$$

The predicted temporal residual state T_t^k consists of two terms, where the first term $R_T \odot \tanh(TF_t^k + HF_t^k)$ represents the encoded features from current input and the second term $R_T \odot ATT_T(\mathcal{T})$ represents the preserved temporal information from previous τ time steps. In this way, more useful temporal information can be kept from a longer past. In particular, $ATT_T(\cdot)$ denotes the temporal attention network which is constructed with convolutional layers and can help merge the multiple temporal states to a single one.

In the spatial module (orange block), by utilizing the multiple spatial states $\mathcal{S} : S_{t-\theta:k-1}^k$, both low-level texture information and high-level semantic information can be jointly utilized, and similar to the temporal module, the state-to-state transitions can be represented as follows,

$$S_t^k = R_S \odot (\tanh(SF_t^k + MF_t^k) + ATT_S(\mathcal{S})), \quad (8)$$

where S_t^k denotes the predicted spatial residual state and ATT_S denotes the spatial attention network.

The predicted temporal residual state T_t^k and the predicted spatial residual state S_t^k will be further aggregated to the final hidden state in the output module (gray block):

$$\begin{aligned} R_O &= \sigma(OF_t^k + HF_t^k + W_{os} * S_t^k + W_{ot} * T_t^k), \\ STRF_t &= R_O \odot \tanh(W_{1 \times 1} * [T_t^k, S_t^k]), \\ STIF_t &= W_{1 \times 1} * [T_E, S_E], \\ H_t^k &= STIF_t^k + STRF_t^k, \end{aligned} \quad (9)$$

where R_O denotes the output residual gate, which is utilized to aggregate the predicted temporal and spatial residual information. H_t^k denotes the final hidden state. In particular, the hidden state H_t^k consists of two terms, where the first term $STIF_t^k$ denotes the spatiotemporal input features and the second term $STRF_t^k$ denotes the predicted spatiotemporal residual features between previous and future frames.

3.3. Training Details

In training stage, to predict more naturalistic results, the proposed model is trained with the help of GANs and the whole model consists of two submodules: predictor P which is utilized to generate future frames and discriminator D which is utilized to judge whether the input frames are real or generated. The adversarial loss for both modules can be expressed as follows,

$$\begin{aligned} \mathcal{L}_{GAN}(D) &= - \sum_{t=2}^T [\log(D(v_t)) + \log(1 - D(\hat{v}_t))], \\ \mathcal{L}_{GAN}(P) &= - \sum_{t=2}^T \log(D(\hat{v}_t)), \end{aligned} \quad (10)$$

where T denotes total number of the time steps. v and \hat{v} denote the input and predicted frames respectively.

Since the discriminators in GANs can model the distribution of the input data (fake or real), we utilize the feature map from the layer k of the discriminator as the learned perceptual representations for current input. And a learned perceptual loss, which can indicate the perceptual distribution of the inputs, is represented as follows (Figure 2),

$$\mathcal{L}_{LP} = \sum_{t=2}^T \mathcal{L}_2[D_k(v_t), D_k(\hat{v}_t)], \quad (11)$$

where D_k denotes the k^{th} layer of the discriminator D (the bottom layer in our method). $\mathcal{L}_2(\cdot)$ denotes the standard MSE loss function. By using the additional loss functions, more naturalistic results can be predicted and the final loss function for the predictor can be expressed as follows,

$$\mathcal{L}_P = \mathcal{L}_{MSE} + \lambda_1 \mathcal{L}_{LP} + \lambda_2 \mathcal{L}_{GAN}(P), \quad (12)$$

where λ_1, λ_2 control the relative importance.

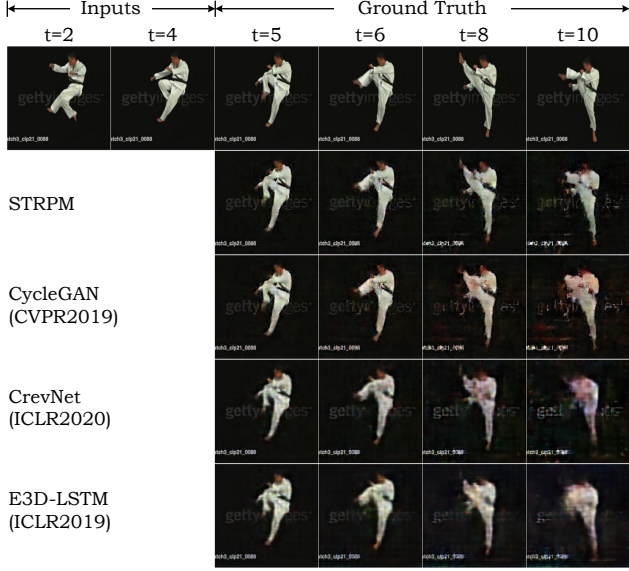


Figure 4. The generated examples on the UCF Sports test set (4 frames \rightarrow 6 frames).

4. Experiments

In this section, we evaluate all models on three high-resolution datasets, UCF Sports dataset (480×720) [19], Human3.6M dataset (1000×1000) [10] and SJTU4K dataset (2160×3840) [21]. We stack 16 RPMs to the proposed STRPM and the integrated convolutional operations are set with a kernel size 5×5 . The stride is set to 1 for each dimension. We set the number of previous spatiotemporal states τ, θ to 5. The hidden states for STRPM and the discriminator are set with 128 channels. All models are implemented using Pytorch and trained with Adam optimizer. In the training stage, models are trained to predict the next frame with 4 successive frames as the input on all datasets. In the testing stage, models are evaluated to predict multiple frames. The balance weights λ_1, λ_2 are set to 0.01, 0.001 for UCF Sports and Human3.6M datasets, and 0.005, 0.0005 for SJTU4K dataset.

4.1. UCF Sports Dataset

The UCF Sports dataset contains a series of human actions collected from various sports events and are typically captured on broadcast television channels such as the BBC and ESPN. A total of 150 videos with resolution of 480×720 are contained in the UCF Sports dataset. We resize each frame to 512×512 . 6,288 sequences are for training and 752 for testing. Figure 4 shows the qualitative results generated from different methods, where the proposed method obviously outperforms others with more naturalistic predictions. In Table 1, we utilize the Peak Signal to Noise Ratio (PSNR) to represent the objective quality and

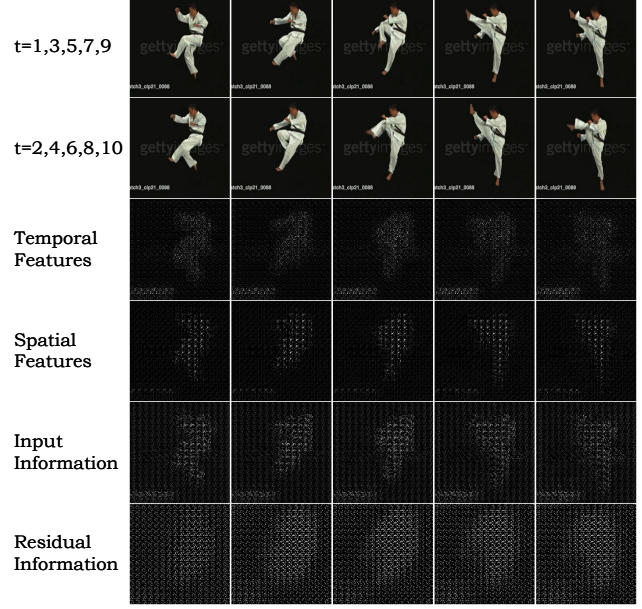


Figure 5. The visualization results of the spatiotemporal encoding scheme and the residual predictive memory. **Temporal Features** and **Spatial Features** denote the encoded features from the temporal encoder and the spatial encoder. **Input Information** and **Residual Information** denote *STIF* and *STRF* in Equation 9.

the Learned Perceptual Image Patch Similarity (LPIPS) [30] to represent the perceptual quality. The quantitative results show that the proposed method achieves the best PSNR score and LPIPS scores.

To further evaluate the efficiency of the proposed spatiotemporal encoding scheme and the residual predictive memory, we visualize the temporal features T_E , the spatial features S_E , the input information and the spatiotemporal residual information (STRF). The visualized results are shown in Figure 5, where the temporal features contain a wider motion area while the spatial features focus on the appearance area of the person with greater weight values. The differences between the temporal features and the spatial features indicate that the spatiotemporal encoding scheme can help extract different features from the temporal domain and the spatial domain, respectively. Moreover, compared with the temporal features, the weights of the learned spatiotemporal residual features are much greater, indicating the proposed residual structure can help the predictive memory pay more attention to modeling the complex motion information instead of the appearance information (the weights of the appearance information is less than the spatial features).

4.2. Human3.6M and SJTU4K Datasets

The Human3.6M dataset consists of 3.6 million 3D human poses and corresponding images acted by 11 profes-

Table 1. Quantitative results of different methods on the UCF Sports (4 frames \rightarrow 6 frames) and Human3.6M (4 frames \rightarrow 4 frames) datasets. Lower LPIPS(10^{-2}) and higher PSNR(dB) scores indicate better results.

Method	UCF Sports		Human3.6M	
	$t = 5$	$t = 10$	$t = 5$	$t = 8$
	PSNR \uparrow / LPIPS \downarrow	PSNR \uparrow / LPIPS \downarrow	PSNR \uparrow / LPIPS \downarrow	PSNR \uparrow / LPIPS \downarrow
BeyondMSE (ICLR2016) [15]	26.42 / 29.01	18.46 / 55.28	-	-
PredRNN (NeurIPS2017) [26]	27.17 / 28.15	19.65 / 55.34	31.91 / 12.62	25.65 / 14.01
PredRNN++ (ICML2018) [24]	27.26 / 26.80	19.67 / 56.79	32.05 / 13.85	27.51 / 14.94
SAVP (arXiv 2018) [13]	27.35 / 25.45	19.90 / 49.91	-	-
SV2P (ICLR2018) [1]	27.44 / 25.89	19.97 / 51.33	31.93 / 13.91	27.33 / 15.02
HFVP (NeurIPS2019) [23]	-	-	32.11 / 13.41	27.31 / 14.55
E3D-LSTM (ICLR2019) [25]	27.98 / 25.13	20.33 / 47.76	32.35 / 13.12	27.66 / 13.95
CycleGAN (CVPR2019) [12]	27.99 / 22.95	19.99 / 44.93	32.83 / 10.18	28.26 / 11.03
CrevNet (ICLR2020) [29]	28.23 / 23.87	20.33 / 48.15	33.18 / 11.54	28.31 / 12.37
MotionRNN (CVPR2021) [27]	27.67 / 24.23	20.01 / 49.20	32.20 / 12.11	28.03 / 13.29
STRPM	28.54 / 20.69	20.59 / 41.11	33.32 / 9.74	29.01 / 10.44

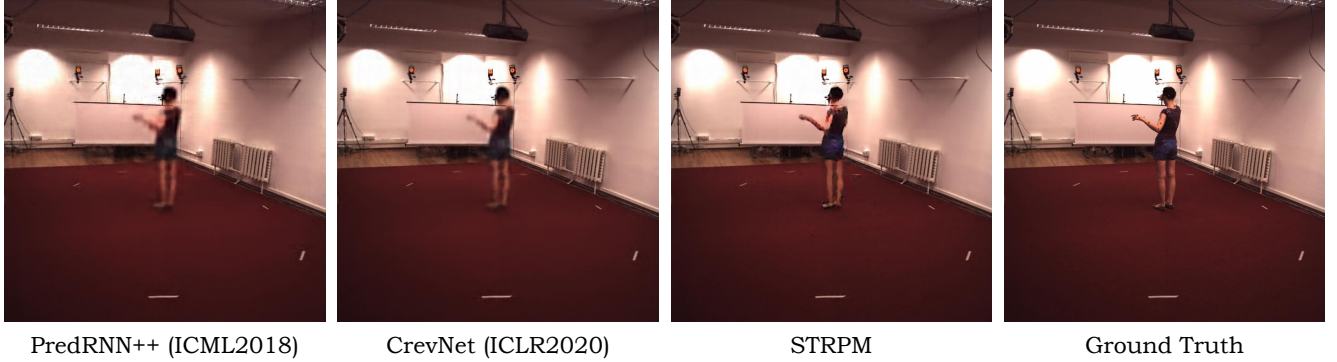


Figure 6. The generated examples on the Human3.6M dataset (4 frames \rightarrow 1 frame).

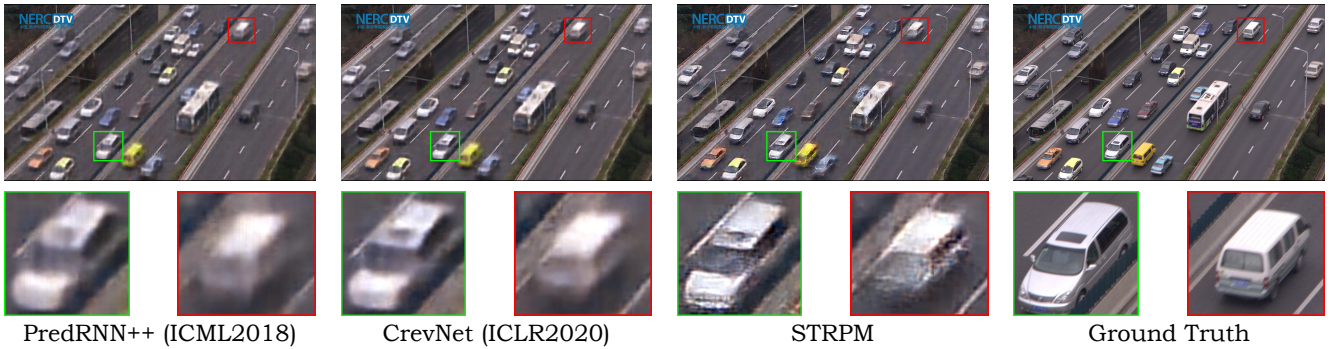


Figure 7. The generated examples on the SJTU4K dataset (4 frames \rightarrow 1 frame).

sional actors in 17 scenarios, including discussion, smoking, taking photos and so on. All videos are recorded with 4 calibrated cameras with a resolution 1000×1000 , which are further resized to 1024×1024 in this paper. 73,404 sequences are for training and 8,582 for testing.

Figure 6 shows the generated examples from the proposed method and other state-of-the-art methods, where the proposed STRPM significantly outperforms others and the predicted results are more naturalistic. In Table 1, the proposed method achieves the best PSNR and LPIPS scores

compared with other state-of-the-art methods.

The SJTU4K dataset consists of 15 ultra-high resolution 4K videos with a wide variety of contents. The resolution for each video is 2160×3840 . To evaluate the performance on ultra-high resolution videos, the inputs and outputs are all 4K videos without being down-sampled. 3,873 sequences are for training and 445 for testing. To the best of our knowledge, the proposed STRPM is the first one predicting 4K videos. Figure 7 shows the predicted 4K video frames from different methods. The quantitative results are summarized in Table 2. As shown in Figure 7 and Table 2, the proposed method has achieved the best qualitative and quantitative results on ultra-high-resolution videos with a satisfactory inference speed.

Table 2. Quantitative results of different methods on the SJTU4K test set (4 frames \rightarrow 4 frames). The inference time over 10 samples have also been summarized.

Method	$t = 5$	$t = 8$	Inference Time
	PSNR \uparrow /LPIPS \downarrow	PSNR \uparrow /LPIPS \downarrow	
ConvLSTM [20]	22.74 / 67.81	17.91 / 86.84	39.38s
PredRNN [26]	23.25 / 66.60	18.20 / 87.04	40.06s
PredRNN++ [24]	23.43 / 64.07	18.55 / 86.34	53.11s
SAVP [13]	23.41 / 61.44	18.63 / 80.45	100.23s
CrevNet [29]	24.35 / 62.31	19.61 / 80.91	52.98s
MotionRNN	23.47 / 65.21	19.72 / 81.39	61.87s
STRPM	24.37 / 57.12	19.77 / 66.68	39.84s

Table 3. Ablation studies on the proposed residual predictive memory and the spatiotemporal encoding-decoding scheme (STED) on the Human3.6M dataset (4 frames \rightarrow 4 frames). PSNR and LPIPS scores are averaged over all 4 predictions. For a fair comparison, the encoders and decoders for all models are with the same structure and the number of the hidden state channels for all the memories is set to 128. We stack 16 memories into each model. All models are trained with MSE loss functions. The floating point operations (FLOPs) are recorded over 1 sample.

Method	PSNR \uparrow	LPIPS \downarrow	Parameters	FLOPs
Casual-LSTM [24]	29.61	14.42	131.35M	36.19G
E3D-LSTM [25]	29.93	13.23	501.37M	128.82G
Reversible-PM [29]	30.13	12.62	114.35M	35.07G
RPM w/o residual	30.11	12.64	108.29M	30.55G
RPM ($\theta = 1, \tau = 1$)	30.14	12.58	45.95M	14.96G
RPM ($\theta = 5, \tau = 1$)	30.56	11.98	77.09M	22.75G
RPM ($\theta = 1, \tau = 5$)	30.32	12.31	77.09M	22.75G
RPM	31.10	11.89	108.29M	30.55G
RPM + STED	31.81	11.72	109.13M	34.24G

Table 4. Ablation studies on STRPM with different loss functions. Performance scores are averaged over all predictions.

Method	UCF sports 4 \rightarrow 6		Human3.6M 4 \rightarrow 4	
	PSNR \uparrow	LPIPS \downarrow	PSNR \uparrow	LPIPS \downarrow
\mathcal{L}_{MSE}	24.89	38.81	31.81	11.72
$\mathcal{L}_{MSE} + \mathcal{L}_{GAN}$	23.98	35.01	30.53	10.98
$\mathcal{L}_{MSE} + \mathcal{L}_{GAN} + \mathcal{L}_{LP}$	24.30	31.50	31.00	10.11

4.3. Ablation Study

In this section, a series of ablation studies are conducted. Table 3 shows the results of different models with different structures. For a fair comparison, all models without STED (the spatiotemporal encoding-decoding scheme) are built with the same structure except the predictive memory. Experimental results show that the proposed residual predictive memory outperforms other state-of-the-art memories with the lowest computation load and fewest parameters. In addition, the residual structure, the broadened temporal receptive field ($\tau > 1$), and the broadened spatial receptive field ($\theta > 1$) can help improve the performance of RPM. Moreover, RPM with STED also help improves the model performance. Furthermore, results from methods trained with different loss functions are summarized in Table 4, where the proposed perceptual loss can help obtain a better trade-off between the objective quality (PSNR) and the perceptual quality (LPIPS).

5. Conclusion and Discussions

We proposed a Spatiotemporal Residual Predictive Model (STRPM) for High-Resolution Video Prediction. We designed the Spatiotemporal Encoding-Decoding Scheme and the Residual Predictive Memory (RPM) to model the much more complex appearance information and motion information in high-resolution videos. In addition, we proposed a Learned Perceptual loss to generate more naturalistic frames compared with the standard MSE loss. Experimental results showed that the proposed model can predict high-resolution videos with the best objective and subjective quality compared with various existing methods.

Although the model performance is better than current methods, the practicality is still far from satisfactory, especially for videos with ultra-high resolutions ($\geq 1080p$). In addition, the model efficiency also needs to be improved for multi-step predictions. Considering the above limitations, current predictive models maybe not reliable enough to be applied into decision-making systems that require data with high accuracy and real-time interactions, such as autonomous driving, robot control, etc. Further works are highly-encouraged to solve the above potential problems.

References

- [1] Mohammad Babaeizadeh, Chelsea Finn, Dumitru Erhan, Roy H Campbell, and Sergey Levine. Stochastic variational video prediction. In *Int. Conf. Learn. Represent.*, 2018. 2, 7
- [2] Apratim Bhattacharyya, Mario Fritz, and Bernt Schiele. Long-term on-board prediction of people in traffic scenes under uncertainty. In *IEEE Conf. Comput. Vis. Pattern Recog.*, pages 4194–4202, 2018. 1
- [3] Zheng Chang, Xinfeng Zhang, Shanshe Wang, Siwei Ma, Yan Ye, and Wen Gao. Stae: A spatiotemporal auto-encoder for high-resolution video prediction. In *Int. Conf. Multimedia and Expo*, pages 1–6. IEEE, 2021. 2
- [4] Xinyuan Chen, Chang Xu, Xiaokang Yang, and Dacheng Tao. Long-term video prediction via criticization and retrospection. *IEEE Trans. Image Process.*, 29:7090–7103, 2020. 2
- [5] Emily Denton and Rob Fergus. Stochastic video generation with a learned prior. In *Int. Conf. Mach. Learn.*, pages 1174–1183, 2018. 2
- [6] Chelsea Finn, Ian Goodfellow, and Sergey Levine. Unsupervised learning for physical interaction through video prediction. In *Adv. Neural Inform. Process. Syst.*, pages 64–72, 2016. 1
- [7] Jean-Yves Franceschi, Edouard Delasalles, Mickaël Chen, Sylvain Lamprier, and Patrick Gallinari. Stochastic latent residual video prediction. In *Int. Conf. Mach. Learn.*, pages 3233–3246. PMLR, 2020. 2
- [8] Ian Goodfellow, Jean Pouget-Abadie, Mehdi Mirza, Bing Xu, David Warde-Farley, Sherjil Ozair, Aaron Courville, and Yoshua Bengio. Generative adversarial nets. In *Adv. Neural Inform. Process. Syst.*, pages 2672–2680, 2014. 2
- [9] Sepp Hochreiter and Jürgen Schmidhuber. Long short-term memory. *Neural Computation*, 9(8):1735–1780, 1997. 2
- [10] Catalin Ionescu, Dragos Papava, Vlad Olaru, and Cristian Sminchisescu. Human3.6m: Large scale datasets and predictive methods for 3d human sensing in natural environments. *IEEE Trans. Pattern Anal. Mach. Intell.*, 2014. 6
- [11] Beibei Jin, Yu Hu, Qiankun Tang, Jingyu Niu, Zhiping Shi, Yinhe Han, and Xiaowei Li. Exploring spatial-temporal multi-frequency analysis for high-fidelity and temporal-consistency video prediction. In *IEEE Conf. Comput. Vis. Pattern Recog.*, pages 4554–4563, 2020. 2
- [12] Yong-Hoon Kwon and Min-Gyu Park. Predicting future frames using retrospective cycle gan. In *IEEE Conf. Comput. Vis. Pattern Recog.*, pages 1811–1820, 2019. 2, 7
- [13] Alex X Lee, Richard Zhang, Frederik Ebert, Pieter Abbeel, Chelsea Finn, and Sergey Levine. Stochastic adversarial video prediction. *arXiv preprint arXiv:1804.01523*, 2018. 2, 7, 8
- [14] Siwei Ma, Xinfeng Zhang, Chuanmin Jia, Zhenghui Zhao, Shiqi Wang, and Shanshe Wang. Image and video compression with neural networks: A review. *IEEE Trans. Circuit Syst. Video Technol.*, 2019. 1
- [15] Michael Mathieu, Camille Couprie, and Yann LeCun. Deep multi-scale video prediction beyond mean square error. In *Int. Conf. Learn. Represent.*, 2016. 2, 7
- [16] Simone Meyer, Abdelaziz Djelouah, Brian McWilliams, Alexander Sorkine-Hornung, Markus Gross, and Christopher Schroers. Phasenet for video frame interpolation. In *IEEE Conf. Comput. Vis. Pattern Recog.*, pages 498–507, 2018. 1
- [17] Simon Niklaus and Feng Liu. Context-aware synthesis for video frame interpolation. In *IEEE Conf. Comput. Vis. Pattern Recog.*, pages 1701–1710, 2018. 1
- [18] MarcAurelio Ranzato, Arthur Szlam, Joan Bruna, Michael Mathieu, Ronan Collobert, and Sumit Chopra. Video (language) modeling: a baseline for generative models of natural videos. *arXiv preprint arXiv:1412.6604*, 2014. 2
- [19] Mikel D Rodriguez, Javed Ahmed, and Mubarak Shah. Action mach a spatio-temporal maximum average correlation height filter for action recognition. In *IEEE Conf. Comput. Vis. Pattern Recog.*, pages 1–8, 2008. 6
- [20] Xingjian Shi, Zhoung Chen, Hao Wang, Dit-Yan Yeung, Wai-Kin Wong, and Wang-chun Woo. Convolutional lstm network: A machine learning approach for precipitation nowcasting. In *Adv. Neural Inform. Process. Syst.*, pages 802–810, 2015. 1, 2, 8
- [21] Li Song, Xun Tang, Wei Zhang, Xiaokang Yang, and Pingjian Xia. The sjtu 4k video sequence dataset. In *International Workshop on Quality of Multimedia Experience*, pages 34–35. IEEE, 2013. 6
- [22] Nitish Srivastava, Elman Mansimov, and Ruslan Salakhudinov. Unsupervised learning of video representations using lstms. In *Int. Conf. Mach. Learn.*, pages 843–852, 2015. 1, 2
- [23] Ruben Villegas, Arkanath Pathak, Harini Kannan, Dumitru Erhan, Quoc V Le, and Honglak Lee. High fidelity video prediction with large stochastic recurrent neural networks. In *Adv. Neural Inform. Process. Syst.*, 2019. 2, 7
- [24] Yunbo Wang, Zhifeng Gao, Mingsheng Long, Jianmin Wang, and S Yu Philip. Predrnn++: Towards a resolution of the deep-in-time dilemma in spatiotemporal predictive learning. In *Int. Conf. Mach. Learn.*, pages 5123–5132, 2018. 2, 7, 8
- [25] Yunbo Wang, Lu Jiang, Ming-Hsuan Yang, Li-Jia Li, Mingsheng Long, and Li. Fei-Fei. Eidetic 3d lstm: A model for video prediction and beyond. In *Int. Conf. Learn. Represent.*, 2019. 1, 7, 8
- [26] Yunbo Wang, Mingsheng Long, Jianmin Wang, Zhifeng Gao, and S Yu Philip. Predrnn: Recurrent neural networks for predictive learning using spatiotemporal lstms. In *Adv. Neural Inform. Process. Syst.*, pages 879–888, 2017. 1, 2, 4, 7, 8
- [27] Haixu Wu, Zhiyu Yao, Jianmin Wang, and Mingsheng Long. Motionrnn: A flexible model for video prediction with spacetime-varying motions. In *IEEE Conf. Comput. Vis. Pattern Recog.*, pages 15435–15444, 2021. 1, 7
- [28] Jingwei Xu, Huazhe Xu, Bingbing Ni, Xiaokang Yang, and Trevor Darrell. Video prediction via example guidance. In *Int. Conf. Mach. Learn.*, pages 10628–10637. PMLR, 2020. 2
- [29] Wei Yu, Yichao Lu, Steve Easterbrook, and Sanja Fidler. Efficient and information-preserving future frame prediction and beyond. In *Int. Conf. Learn. Represent.*, 2020. 1, 2, 7, 8

- [30] Richard Zhang, Phillip Isola, Alexei A Efros, Eli Shechtman, and Oliver Wang. The unreasonable effectiveness of deep features as a perceptual metric. In *IEEE Conf. Comput. Vis. Pattern Recog.*, pages 586–595, 2018. [6](#)
- [31] Jun-Yan Zhu, Taesung Park, Phillip Isola, and Alexei A Efros. Unpaired image-to-image translation using cycle-consistent adversarial networks. In *Int. Conf. Comput. Vis.*, pages 2223–2232, 2017. [2](#)